

Second-order Semi-implicit Projection Methods for Landau-Lifshitz Equation

Changjian Xie

*School of Mathematical Sciences
Soochow University, Suzhou, China*

Joint work with

Jingrun Chen (Soochow University)
Cheng Wang (University of Massachusetts)

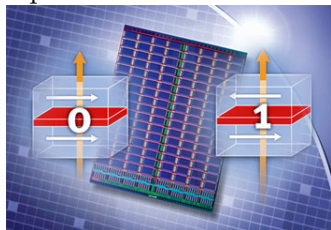
December 8, 2018, Nanjing

- 1 Background and motivation
- 2 Semi-implicit projection methods
- 3 Main theoretical results
 - Unconditional unique solvability
 - Optimal rate convergence analysis
- 4 Numerical examples
- 5 Conclusion

- 1 Background and motivation
- 2 Semi-implicit projection methods
- 3 Main theoretical results
 - Unconditional unique solvability
 - Optimal rate convergence analysis
- 4 Numerical examples
- 5 Conclusion

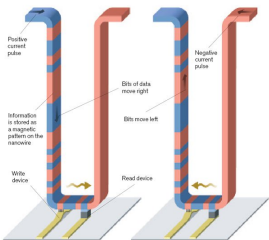
Magnetic recording devices and computer storages

- Spinvalues¹



Magnetoresistance random access memory (MRAM)

- Domain walls²



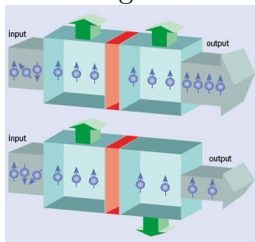
Racetrack memories

¹Science@Berkeley Lab: The Current Spin on Spintronics

²<http://www2.technologyreview.com/article/412189/tr10-racetrack-memory/>

Methodology for detecting the orientation

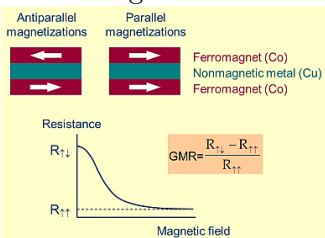
● Tunnel magnetoresistance ³



Julliere's model:
Constant tunneling
matrix

$$\text{TMR} \equiv \frac{G_{\text{AP}} - G_{\text{P}}}{G_{\text{AP}}} = \frac{2P_{\text{L}}P_{\text{R}}}{1 - P_{\text{L}}P_{\text{R}}}$$
$$P_{\text{L}} = \frac{n_{\text{L}}^{\uparrow} - n_{\text{L}}^{\downarrow}}{n_{\text{L}}^{\uparrow} + n_{\text{L}}^{\downarrow}} \quad P_{\text{R}} = \frac{n_{\text{R}}^{\uparrow} - n_{\text{R}}^{\downarrow}}{n_{\text{R}}^{\uparrow} + n_{\text{R}}^{\downarrow}}$$

● Giant magnetoresistance ⁴



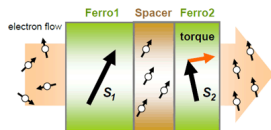
- ▶ Albert Fert and Peter Gruber: 2007 Nobel Prize in Physics
- ▶ Polarization and scattering

³<http://ducthe.wordpress.com/category/spintronics/>

⁴<http://physics.unl.edu/>

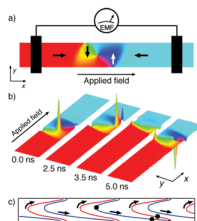
Methodology for rotating the orientation

- Spin transfer torque (STT) ⁵



- ▶ Two layers of different thickness: different switching fields
- ▶ The thin film is switched, and the resistance measured

- Current-driven domain wall motion ⁶



- ▶ Applied current supplies spin transfer torques

⁵http://www.wpi-aimr.tohoku.ac.jp/miyazaki_lab/spintorque.htm

⁶<http://physics.aps.org/articles/v2/11>

Basic quantity of interest:

$$\mathbf{m} : \Omega \longrightarrow \mathbb{R}^3; \quad |\mathbf{m}| = 1$$

Landau-Lifshitz energy functional:

$$\begin{aligned} F_{\text{LL}}[\mathbf{m}] &= \frac{K_u}{M_s} \int_{\Omega} \phi(\mathbf{m}) \, dx + \frac{C_{\text{ex}}}{M_s} \int_{\Omega} |\nabla \mathbf{m}|^2 \, dx \\ &\quad - \frac{\mu_0}{2} M_s \int_{\Omega} \mathbf{h}_s \cdot \mathbf{m} \, dx - \mu_0 M_s \int_{\Omega} \mathbf{h}_e \cdot \mathbf{m} \, dx \end{aligned}$$

- Continuum theory.
- Domain structure \longleftrightarrow Local minimizers.

- Torque balance

$$\mathbf{m}_t = -\mathbf{m} \times \mathbf{h} + \alpha \mathbf{m} \times \mathbf{m}_t,$$

or equivalently,

$$\mathbf{m}_t = -\frac{1}{1 + \alpha^2} \mathbf{m} \times \mathbf{h} - \frac{\alpha}{1 + \alpha^2} \mathbf{m} \times (\mathbf{m} \times \mathbf{h}),$$

where

$$\mathbf{h} = -\frac{\delta F_{LL}}{\delta \mathbf{m}} = -Q(m_2 \mathbf{e}_2 + m_3 \mathbf{e}_3) + \epsilon \Delta \mathbf{m} + \mathbf{h}_s + \mathbf{h}_e$$

and the second term is the Gilbert damping term.

- $\alpha \ll 1$: Damping coefficient

$$\mathbf{m}_t = -\mathbf{m} \times \Delta \mathbf{m} + \alpha \mathbf{m} \times \mathbf{m}_t,$$

or

$$\mathbf{m}_t = -\mathbf{m} \times \Delta \mathbf{m} - \alpha \mathbf{m} \times (\mathbf{m} \times \Delta \mathbf{m})$$

with the Neumann boundary condition and the constraint $|\mathbf{m}| = 1$.

Review articles: [Kružík and Prohl, 2006; Cimrák, 2008]

- Finite element: [Bartels and Prohl, 2006; Alouges, 2008; Cimrák, 2009];
- Finite difference: [E and Wang, 2001; Fuwa et al., 2012; Kim and Lipnikov, 2017];

Linearity of the discrete system:

- Explicit scheme: [Jiang et al., 2001; Alouges and Jaisson, 2006];
- Fully implicit scheme: [Prohl, 2001; Bartels and Prohl, 2006; Fuwa et al., 2012];
- Semi-implicit scheme: [Wang, Garcia-Cervera, and E, 2001; E and Wang, 2001; Gao, 2014; Lewis and Nigam, 2003; Cimrák, 2005].

Time marching

- Splitting method: [Wang, Garcia-Cervera, and E, 2001];
- Mid-point method: [Bertotti et al., 2001, d'Aquino et al., 2005];
- Runge-Kutta methods: [Romeo et al., 2008];
- Geometric integration methods: [Jiang, Kaper, and Leaf, 2001];

Convergence analysis

- 1st order in time + 2nd order in space: [Alouges, 2008];
- 2st order in time + 2nd order in space: [Bertotti et al., 2001, d'Aquino et al., 2005, Bartels and Prohl, 2006, Fuwa et al., 2012];
 - ▶ Unconditional stability;
 - ▶ Nonlinear solver at each time step (unavailable theoretical justification of the unique solvability);
 - ▶ Step-size condition $k = \mathcal{O}(h^2)$ with k the temporal stepsize and h the spatial stepsize;

Outline

- 1 Background and motivation
- 2 Semi-implicit projection methods
- 3 Main theoretical results
 - Unconditional unique solvability
 - Optimal rate convergence analysis
- 4 Numerical examples
- 5 Conclusion

Spatial discretization

- $x_i = ih$, $i = 0, 1, 2, \dots, N_x$, with $x_0 = 0$, $x_{N_x} = 1$;
- $\hat{x}_i = x_{i-1/2} = (i - 1/2)h$, $i = 1, \dots, N_x$;
- $\mathbf{m}_i^n \approx \mathbf{m}(\hat{x}_i, t^n)$;
- $\Delta_h \mathbf{m}_i = \frac{\mathbf{m}_{i+1} - 2\mathbf{m}_i + \mathbf{m}_{i-1}}{h^2}$;
- Third order extrapolation for boundary condition:

$$\mathbf{m}_1 = \mathbf{m}_0, \quad \mathbf{m}_{N_x+1} = \mathbf{m}_{N_x}.$$

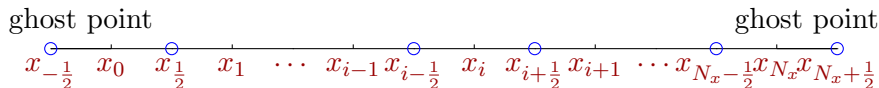


Figure 1: Illustration of the 1-D spatial mesh.

Semi-implicit projection methods [Xie, Garcia-Cervera, Wang, Zhou, and Chen, in progress, 2018]

- $\mathbf{m}_t = -\mathbf{m} \times \Delta \mathbf{m} + \alpha \mathbf{m} \times \mathbf{m}_t$:

$$(1 - \alpha \hat{\mathbf{m}}_h^{n+2} \times) \frac{\frac{3}{2} \mathbf{m}_h^{n+2} - 2 \mathbf{m}_h^{n+1} + \frac{1}{2} \mathbf{m}_h^n}{k} = -\hat{\mathbf{m}}_h^{n+2} \times \Delta_h \mathbf{m}_h^{n+2},$$
$$\hat{\mathbf{m}}_h^{n+2} = 2 \mathbf{m}_h^{n+1} - \mathbf{m}_h^n;$$

- $\mathbf{m}_t = -\mathbf{m} \times \Delta \mathbf{m} - \alpha \mathbf{m} \times (\mathbf{m} \times \Delta \mathbf{m})$:

$$\frac{\frac{3}{2} \mathbf{m}_h^{n+2} - 2 \mathbf{m}_h^{n+1} + \frac{1}{2} \mathbf{m}_h^n}{k} = -\hat{\mathbf{m}}_h^{n+2} \times \Delta_h \mathbf{m}_h^{n+2}$$
$$- \alpha \hat{\mathbf{m}}_h^{n+2} \times (\hat{\mathbf{m}}_h^{n+2} \times \Delta_h \mathbf{m}_h^{n+2});$$

- A projection step: $\mathbf{m}_h^{n+2} = \frac{\mathbf{m}_h^{n+2}}{|\mathbf{m}_h^{n+2}|}$.

1D test: Accuracy

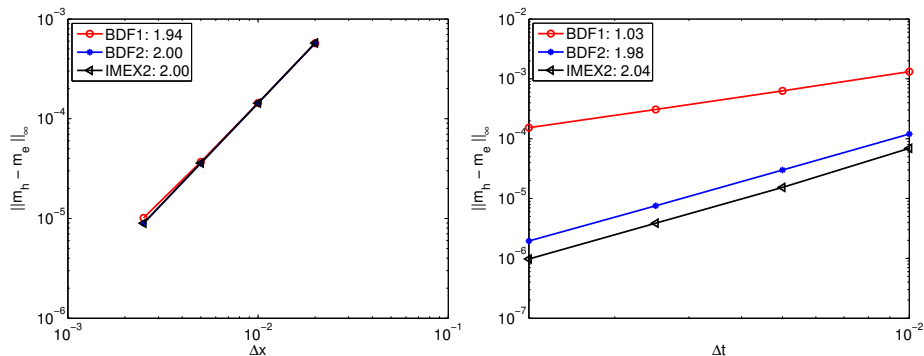


Figure 2: Accuracy of BDF1, BDF2, and IMEX2. They are all second-order accurate in space. BDF1 is first-order accurate in time. BDF2 and IMEX2 are second-order accurate in time.

1D test: Efficiency

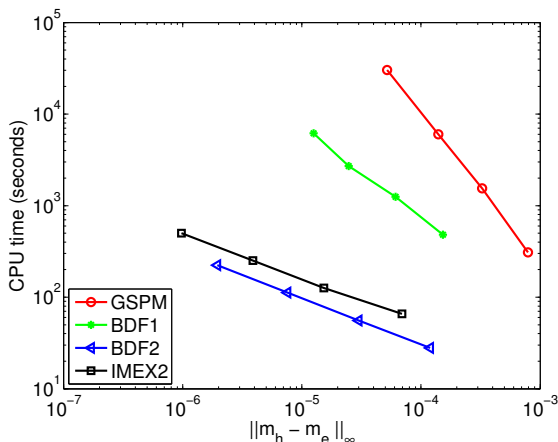


Figure 3: CPU time (in seconds) of GSPM, BDF1, BDF2, and IMEX2 versus error $\|m_h - m_e\|_\infty$. For a given tolerance of error, costs of these schemes in the increasing order are: BDF2 < IMEX2 < BDF1 < GSPM.

- Lack of numerical stability of Lax-Richtmyer type;
- Separation of the time-marching step and the projection step:

$$\begin{aligned}\frac{\frac{3}{2}\tilde{\mathbf{m}}_h^{n+2} - 2\tilde{\mathbf{m}}_h^{n+1} + \frac{1}{2}\tilde{\mathbf{m}}_h^n}{k} &= -\hat{\mathbf{m}}_h^{n+2} \times \Delta_h \tilde{\mathbf{m}}_h^{n+2} \\ &\quad - \alpha \hat{\mathbf{m}}_h^{n+2} \times (\hat{\mathbf{m}}_h^{n+2} \times \Delta_h \tilde{\mathbf{m}}_h^{n+2}), \\ \hat{\mathbf{m}}_h^{n+2} &= 2\mathbf{m}_h^{n+1} - \mathbf{m}_h^n, \\ \mathbf{m}_h^{n+2} &= \frac{\tilde{\mathbf{m}}_h^{n+2}}{|\tilde{\mathbf{m}}_h^{n+2}|};\end{aligned}$$

- Two sets of approximations $\tilde{\mathbf{m}}_h^n$ and \mathbf{m}_h^n .

$$\mathbf{m}_e = (\cos(x^2(1-x)^2) \sin t, \sin(x^2(1-x)^2) \sin t, \cos t)^T$$

Table 1: Accuracy of our method on the uniform mesh when $h = k$ and $\alpha = 0.01$.

k	$\ \mathbf{m}_h - \mathbf{m}_e\ _\infty$	$\ \mathbf{m}_h - \mathbf{m}_e\ _2$	$\ \mathbf{m}_h - \mathbf{m}_e\ _{H^1}$
2.0D-2	4.990D-5	5.865D-5	1.060D-4
1.0D-2	1.262D-5	1.434D-5	2.666D-5
5.0D-3	3.167D-6	3.545D-6	6.762D-6
2.5D-3	7.927D-7	8.813D-7	1.699D-6
1.25D-3	1.983D-7	2.197D-7	4.257D-7
6.25D-4	4.961D-8	5.484D-8	1.065D-7
order	1.996	2.012	1.991

- 1 Background and motivation
- 2 Semi-implicit projection methods
- 3 Main theoretical results**
 - Unconditional unique solvability
 - Optimal rate convergence analysis
- 4 Numerical examples
- 5 Conclusion

Unconditional unique solvability

Theorem

Given \mathbf{p}_h , $\hat{\mathbf{m}}_h$, the numerical scheme

$$\frac{\frac{3}{2}\tilde{\mathbf{m}}_h - \mathbf{p}_h}{k} = -\hat{\mathbf{m}}_h \times \Delta_h \tilde{\mathbf{m}}_h - \alpha \hat{\mathbf{m}}_h \times (\hat{\mathbf{m}}_h \times \Delta_h \tilde{\mathbf{m}}_h)$$

is uniquely solvable.

Denote $\mathbf{q}_h = -\Delta_h \tilde{\mathbf{m}}_h$. Then

$$\tilde{\mathbf{m}}_h = (-\Delta_h)^{-1} \mathbf{q}_h + C_{\mathbf{q}_h}^* \quad \text{with} \quad C_{\mathbf{q}_h}^* = \frac{2}{3} \left(\overline{\mathbf{p}_h + k \hat{\mathbf{m}}_h \times \mathbf{q}_h + \alpha k \hat{\mathbf{m}}_h \times (\hat{\mathbf{m}}_h \times \mathbf{q}_h)} \right)$$

and

$$G(\mathbf{q}_h) := \frac{\frac{3}{2}((- \Delta_h)^{-1} \mathbf{q}_h + C_{\mathbf{q}_h}^*) - \mathbf{p}_h}{k} - \hat{\mathbf{m}}_h \times \mathbf{q}_h - \alpha \hat{\mathbf{m}}_h \times (\hat{\mathbf{m}}_h \times \mathbf{q}_h) = \mathbf{0}.$$

Lemma (Browder-Minty lemma [Browder, 1963, Minty, 1963])

Let X be a real, reflexive Banach space and let $T : X \rightarrow X'$ (the dual space of X) be bounded, continuous, coercive (i.e., $\frac{(T(u), u)}{\|u\|_X} \rightarrow +\infty$, as $\|u\|_X \rightarrow +\infty$) and monotone. Then for any $g \in X'$ there exists a solution $u \in X$ of the equation $T(u) = g$. Furthermore, if the operator T is strictly monotone, then the solution u is unique.

By the Browder-Minty lemma, the semi-implicit scheme admits a unique solution.

Theorem

Let $\mathbf{m}_e \in C^3([0, T]; C^0) \cap L^\infty([0, T]; C^4)$ be a smooth solution with the initial data $\mathbf{m}_e(\mathbf{x}, 0) = \mathbf{m}_e^0(\mathbf{x})$ and \mathbf{m}_h be the numerical solution with the initial data $\mathbf{m}_h^0 = \mathbf{m}_{e,h}^0$ and $\mathbf{m}_h^1 = \mathbf{m}_{e,h}^1$. Suppose that the initial error satisfies

$$\|\mathbf{m}_{e,h}^\ell - \mathbf{m}_h^\ell\|_2 + \|\nabla_h(\mathbf{m}_{e,h}^\ell - \mathbf{m}_h^\ell)\|_2 = \mathcal{O}(k^2 + h^2), \quad \ell = 0, 1, \text{ and } k \leq Ch.$$

Then the following convergence result holds as h and k goes to zero:

$$\|\mathbf{m}_{e,h}^n - \mathbf{m}_h^n\|_2 + \|\nabla_h(\mathbf{m}_{e,h}^n - \mathbf{m}_h^n)\|_2 \leq C(k^2 + h^2), \quad \forall n \geq 2,$$

in which the constant $C > 0$ is independent of k and h .

Idea of the proof

$$\begin{array}{ccccccc} \|\tilde{\mathbf{e}}_h^2\|, \|\nabla_h \tilde{\mathbf{e}}_h^2\| & & \|\tilde{\mathbf{e}}_h^3\|, \|\nabla_h \tilde{\mathbf{e}}_h^3\| & & \|\tilde{\mathbf{e}}_h^4\|, \|\nabla_h \tilde{\mathbf{e}}_h^4\| & & \dots \\ & \uparrow & & \uparrow & & \uparrow & \\ \|\mathbf{e}_h^0\|, \|\nabla_h \mathbf{e}_h^0\| & \dashrightarrow & \|\mathbf{e}_h^1\|, \|\nabla_h \mathbf{e}_h^1\| & \dashrightarrow & \|\mathbf{e}_h^2\|, \|\nabla_h \mathbf{e}_h^2\| & \dashrightarrow & \|\mathbf{e}_h^3\|, \|\nabla_h \mathbf{e}_h^3\| & \dots \end{array}$$

Blue arrow (Lemma)

Red arrow (Discrete Gronwall Inequality)

Dashed arrow (Combine these terms)

Lemma

Consider $\underline{\mathbf{m}}_h = \mathbf{m}_e + h^2 \mathbf{m}^{(1)}$ with \mathbf{m}_e the exact solution and $|\mathbf{m}_e| = 1$ at a point-wise level, and $\|\mathbf{m}^{(1)}\|_\infty + \|\nabla_h \mathbf{m}^{(1)}\|_\infty \leq \mathcal{C}$. For any numerical solution $\tilde{\mathbf{m}}_h$, we define $\mathbf{m}_h = \frac{\tilde{\mathbf{m}}_h}{|\tilde{\mathbf{m}}_h|}$. Suppose both numerical profiles satisfy the following $W_h^{1,\infty}$ bounds

$$|\tilde{\mathbf{m}}_h| \geq \frac{1}{2}, \quad \text{at a point-wise level,}$$

$$\|\mathbf{m}_h\|_\infty + \|\nabla_h \mathbf{m}_h\|_\infty \leq M, \quad \|\tilde{\mathbf{m}}_h\|_\infty + \|\nabla_h \tilde{\mathbf{m}}_h\|_\infty \leq M,$$

and we denote the numerical error functions as $\mathbf{e}_h = \underline{\mathbf{m}}_h - \mathbf{m}_h$, $\tilde{\mathbf{e}}_h = \underline{\mathbf{m}}_h - \tilde{\mathbf{m}}_h$. Then the following estimate is valid

$$\|\mathbf{e}_h\|_2 \leq 2\|\tilde{\mathbf{e}}_h\|_2 + \mathcal{O}(h^2), \quad \|\nabla_h \mathbf{e}_h\|_2 \leq \mathcal{C}(\|\nabla_h \tilde{\mathbf{e}}_h\|_2 + \|\tilde{\mathbf{e}}_h\|_2) + \mathcal{O}(h^2).$$

Verification of assumptions.

$$|\tilde{\mathbf{m}}_h| \geq \frac{1}{2}, \quad \text{at a point-wise level,}$$

$$\|\mathbf{m}_h\|_\infty + \|\nabla_h \mathbf{m}_h\|_\infty \leq M, \quad \|\tilde{\mathbf{m}}_h\|_\infty + \|\nabla_h \tilde{\mathbf{m}}_h\|_\infty \leq M,$$

$$\|\mathbf{e}_h^n\|_\infty \leq \frac{1}{6}, \quad \|\nabla_h \mathbf{e}_h^n\|_\infty \leq \frac{1}{6},$$

$$\|\tilde{\mathbf{e}}_h^n\|_\infty \leq \frac{1}{6}, \quad \|\nabla_h \tilde{\mathbf{e}}_h^n\|_\infty \leq \frac{1}{6}.$$



Outline

- 1 Background and motivation
- 2 Semi-implicit projection methods
- 3 Main theoretical results
 - Unconditional unique solvability
 - Optimal rate convergence analysis
- 4 Numerical examples
- 5 Conclusion

Homogenous Neumann boundary condition

- 1 1-D example with a forcing term and the given exact solution
- 2 1-D example without the exact solution
- 3 3-D example with a forcing term and the given exact solution

Example 1

$$\mathbf{m}_e = (\cos(x^2(1-x)^2) \sin t, \sin(x^2(1-x)^2) \sin t, \cos t)^T$$

Table 2: Accuracy of our method on the uniform mesh when $h = k$ and $\alpha = 0.01$.

k	$\ \mathbf{m}_h - \mathbf{m}_e\ _\infty$	$\ \mathbf{m}_h - \mathbf{m}_e\ _2$	$\ \mathbf{m}_h - \mathbf{m}_e\ _{H^1}$
2.0D-2	4.990D-5	5.865D-5	1.060D-4
1.0D-2	1.262D-5	1.434D-5	2.666D-5
5.0D-3	3.167D-6	3.545D-6	6.762D-6
2.5D-3	7.927D-7	8.813D-7	1.699D-6
1.25D-3	1.983D-7	2.197D-7	4.257D-7
6.25D-4	4.961D-8	5.484D-8	1.065D-7
order	1.996	2.012	1.991

Example 2

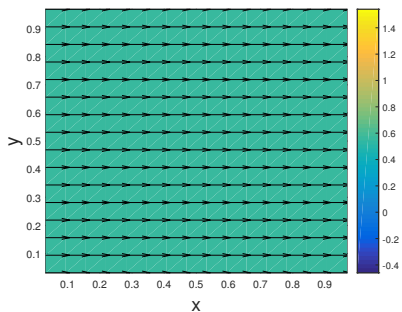
Table 3: Temporal accuracy of our method on the uniform mesh when $h = 5D - 5$ and $\alpha = 0.01$.

k	$\ \mathbf{m}_h - \mathbf{m}_e\ _\infty$	$\ \mathbf{m}_h - \mathbf{m}_e\ _2$	$\ \mathbf{m}_h - \mathbf{m}_e\ _{H^1}$
4.0D-2	5.778D-4	5.284D-4	0.00168
2.0D-2	1.456D-4	1.347D-4	4.095D-4
1.0D-2	3.652D-5	3.399D-5	1.010D-4
5.0D-3	9.147D-6	8.535D-6	2.523D-5
2.5D-3	2.287D-6	2.136D-6	6.640D-6
order	1.996	1.988	1.999

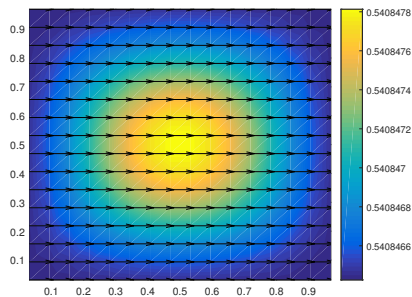
Table 4: Spatial accuracy of our method on the uniform mesh when $k = 1D - 4$ and $\alpha = 0.01$.

h	$\ \mathbf{m}_h - \mathbf{m}_e\ _\infty$	$\ \mathbf{m}_h - \mathbf{m}_e\ _2$	$\ \mathbf{m}_h - \mathbf{m}_e\ _{H^1}$
$1/3^2$	0.00546	0.00577	0.01336
$1/3^3$	6.101D-4	6.430D-4	0.0016
$1/3^4$	6.783D-5	7.147D-5	1.821D-4
$1/3^5$	7.536D-6	7.940D-6	2.038D-5
$1/3^6$	8.363D-7	8.811D-7	2.268D-6
order	1.999	2.000	1.978

Example 3



(a) Exact magnetization profile



(b) Numerical magnetization profile

Figure 4: Profiles of the exact and the numerical magnetization in the xy -plane with $z = 1/2$ when $k = 1/16$, $h_x = h_y = h_z = 1/16$, and $\alpha = 0.01$.

Table 5: Temporal accuracy in the 3-D case when $h_x = h_y = h_z = 1/16$ and $\alpha = 0.01$.

k	$\ \mathbf{m}_h - \mathbf{m}_e\ _\infty$	$\ \mathbf{m}_h - \mathbf{m}_e\ _2$	$\ \mathbf{m}_h - \mathbf{m}_e\ _{H^1}$
1/8	0.00360	0.00237	0.00233
1/16	9.983D-4	6.544D-4	6.612D-4
1/32	2.583D-4	1.691D-4	1.708D-4
1/64	6.256D-5	4.077D-4	4.164D-5
1/128	1.234D-5	7.846D-6	8.663D-6
order	2.047	2.059	2.018

- 1 Background and motivation
- 2 Semi-implicit projection methods
- 3 Main theoretical results
 - Unconditional unique solvability
 - Optimal rate convergence analysis
- 4 Numerical examples
- 5 Conclusion

What we have done

- ① Several second-order semi-implicit schemes for LL equation;
- ② Convergence analysis for one of the schemes.

To-do list

- ① Benchmark problem from NIST (in progress);
- ② Generalization of the technique for other implicit scheme;
- ③ Current-driven magnetization dynamics [Chen, Garcia-Cervera, and Yang, 2015].

Thank you for your attention!